I.A.U. Karaj Branch

Journal of Applied Chemical Research, 11, 1, 45-62 (2017)

Journal of Applied Chemical Research
www.jacr.kiau.ac.ir

Interaction of Human Serum Albumin with Ethyl 2-[2-(dimethylamino)-4-(4-nitrophenyl)-1,3-thiazole-5-yl]-2-oxoacetate as a Synthesized Ligand

Mahboube Eslami Moghadam[1*], Maryam Saidifar[2], Faramarz Rostami-Charati[3*], Zinatossadat Hossaini [4], Maryam Ghadamgahi[5]

[1]Chemistry & Chemical Engineering Research Center of Iran, Tehran, Iran

[2]Nanotechnology and Advanced Materials Department, Materials and Energy Research Center, Karaj, Iran

[3]Department of Chemistry, Facualty of Science, Gonbad Kavous University, Gonbad, Iran

[4]Department of Chemistry, Qaemshahr Branch, Islamic Azad University, Qaemshahr, Iran

[5]School of Chemistry, Damghan University, Damghan, Iran

(Received 14 Jul. 2016; Final version received 18 Sep. 2016)

Abstract

The interaction of human serum albumin with Ethyl 2-[2-(dimethylamino)-4-(4-nitrophenyl)-1,3-thiazole-5-yl]-2-oxoacetate was investigated by using isothermal titration UV-visible spectrophotometry in tris-buffer, pH 7.4. According to these results, it was found that there are a set of 4 binding sites for this ligand on HSA with positive cooperativity in the binding process. This thiazole derivative can denature the protein as surfactants. Also, their binding was investigated by molecular dynamics simulation in combination with molecular docking. Parameters of surface area, radius of gyration, hydrogen bonding, RMSD, potential of mean force, diffusion coefficient, radial distribution function, helix and coil structures were obtained. It was observed that surfactant reduce intermolecular hydrogen bond and unfold HSA structure more at higher temperature.

***Keywords**: 1, 3-Thiazole, Isothermal titration, HSA denaturation, Thermodynamic, Molecular docking.*

Introduction

The modification of anticancer drugs structure and determination of the influence of chemical structure on their biological activity have developed medicinal chemistry, especially chemotherapy chemistry and side effects

***Corresponding author:** Mahboube Eslami-Moghadam, Chemistry & Chemical Engineering Research Center of Iran. Tehran, Iran. Tel.: +982144787772; Fax: +982144787753E-mail address: eslami_moghadam@yahoo.com & eslami_moghadam@ccerci.ac.ir.*

reduction. Hence, the design and synthesis of new derivatives of anticancer drugs could be assisted with the interpretation and the identification of mechanism of action of biologically active compounds and determination of their binding modes at the molecular level [1, 2]. On the other hand, human serum albumin is the carrier protein in human blood. HSA has a high ability to bind metal ions, drugs, fatty acids, hormones, and other compounds and transports them because the hydrophobic sections in the protein is available and flexible. Thus, studying on the interaction of HSA with some organic compound is very important to detect probable side effects [3-6]. Moreover some compound as drug may interact with varieties of proteins inside or outside the cell creating unknown problems. Thus, binding studies of such agents with proteins are equally important as their DNA-interaction studies [7].

In this paper we are reporting the interaction of Ethyl 2-[2-(dimethylamino)-4-(4-nitrophenyl)-1,3-thiazole-5-yl]-2-oxoacetate with human serum albumin by applying molecular dynamics, molecular docking and Spectroscopic Studies. This study confirms good ability of molecular docking and molecular dynamics results combination to agree with experimental data. It emphasis in great unfolding influence of studied surfactant on HSA, and also concentrates on the interaction of this ligand at two temperatures by molecular dynamics simulation that is a valid method to describe and investigate ligand-protein interaction.

HSA-binding studies

Determination of binding parameter of the protein interaction with ligand was done similar to the reported spectral methods [8-12]. The stock solution of HSA (0.8 mg/ml) was prepared by dissolving in Tris-HCl buffer by gentle stirring at room temperature. Using extinction coefficient of 66.7 $cm^{-1}mM^{-1}$ for protein solution, the concentration of HSA was measured the absorbance at 280 nm [13]. Ligand stock concentration (0.1 mmol/L) was also prepared with double distilled water and the spectrophotometric readings at λ_{max} of this ligand (~310 nm), where HSA has no absorption, were recorded.

Spectrophotometry for protein denaturation study

In this experiment, the sample cell containing 1.8 mL 0.8 mg/mL HSA that the absorption HSA is around 0.4, was incubated with 10 µl ligand injections to 2 ml volume cell where the concentration was being 0 to 0.01 mmol/L. The absorption of the sample cells was recorded at 280 nm versus the reference cells at two constant temperatures, 27 or 37 oC, separately. Also, the concentration of ligand for protein denaturation, $[L]_{1/2}$, and thermodynamic parameters were found out

using Pace method [14, 15].

Spectrophotometry for ligand binding study

The protein-ligand interaction was investigated by applying isothermal titration method [15]. With (2.5-4.5 μmol/L) with HSA (0.8 mg/ml) was titrated with different concentrations of ligand and incubated for 30 min at 27 or 37 ^{o}C, separately. Then, the spectrophotometric readings at 310 nm were recorded. When all the binding sites on HSA were bound by ligand, the binding parameters of ligand with HAS [16-18], where n is Hill coefficient, g is the number of binding sites and K is apparent binding constant and the other thermodynamic binding were determined according to reported method [18]. All measurements were performed separately at 27 and 37 °C and were repeated three times for each experiment.

Fluorescence quenching measurements

The protein fluorescence quenching effect of mentioned ligand was carried out by using Fluorescence spectroscopy and data were recorded on FP-6200 Jasco fluorescence spectrophotometer. In this study, HSA was excited at 295 nm and the emission spectra were recorded between 300 and 400 nm in the absence and presence of different concentrations of ligand. Every time, 10 μL of 5 μM ligand stock solution was injected into the HSA solution (2 ml of 5 μM) in Tris-HCl buffer and Changes in the maximum fluorescence emission of protein were recorded at room temperature.

Experimental

Apparatus and analysis

Human serum albumin (HSA) was purchased from Sigma-Aldrich. Commercially pure chemicals of Tris-HCl buffer, sodium chloride, sodium hydroxide, hydrochloric acid, were purchased from Merck Germany. Ligand was synthesized in the laboratory (Scheme 1). Electronic absorption spectra of ligand-HSA interactions were measured on a Jenwey UV-6800 recording spectrophotometer. All solutions were made in double-distilled water. 10 mmol/L Tris-HCl solution (10 mmol/L NaCl, pH 7.4) was used as a buffer.

Ethyl 2-[2-(dimethylamino)-4-(4-nitrophenyl) -1,3-thiazole-5-yl]-2-oxoacetate.

Yellow crystals, Yield: 0.63 g (90%), m.p. 122-124°C. IR (KBr) (ν_{max}/cm^{-1}): 1741, 1714, 1690, 1631 cm^{-1}. ^{1}H NMR: 0.99 (t, 3 H, ^{3}J = 7.2, Me), 3.21 (s, 6 H, NMe2), 3.82 (q, 2 H, ^{3}J = 7.2, OCH_2), 7.85 (d, 2 H, ^{3}J = 8.6, 2 CH), 8.25 (d, 2 H, ^{3}J = 8.6, 2 CH). ^{13}C NMR: 13.6 (Me), 40.5 (NMe_2), 62.0 (OCH_2), 123.6 (2 CH), 125.9 (C), 129.2 (2 CH), 144.3 (C), 149.6 (C), 149.7 (C), 162.8, 172.6, 185.1 (C-2 and 2 C=O). EI-MS: 349 (M^+, 15), 304 (48), 227 (64), 122 (100), 45 (86), 44 (56). Anal. Calcd for $C_{15}H_{15}N_3O_5S$ (349.35): C 51.57, H 4.33, N 12.03, Found: C 51.81, H 4.26, N

12.10; UV band maxima in nm (εm in liter mole^{-1} cm^{-1} 10-3): 309 (7.46), 273 (6.59), 230 (5.55), 205 (4.95).

Molecular dynamic simulation

All calculations are carried out by a multicore computer which has Intel(R) Pentium(R) Dual CPU with 4 GB RAM. GROMACS software version 3.3.1 [19] was used for simulation. The structure of Ethyl 2-[2-(dimethylamino)-4-(4-nitrophenyl)-1,3-thiazole-5-yl]-2-oxoacetate was optimized using Hyperchem 7 software with Molecular Mechanics Force Field (MM+). Semi-empirical AM1 was set up as optimization method. Free online PRODRG2 server (http://davapc1.bioch.dundee.ac.uk/cgi-bin/prodrg_beta) was used to generate topology of ligand. HSA structure with pdb id code of 1AO6 was constructed by protein data bank. GROMOSE96 53a6 force field with SPC216 model was used to create ligand-protein and solvent parameters. Five ligands were located around the HSA in similar position and after water addition; the system was run 20 ns. The temperature was controlled by Nose-Hoover thermostat at 300 and 310 K and the pressure was adjusted at 1 bar by Parrinello-Rahman barostat. All bonds were restrained by LINC algorithm. Particle-Mesh Ewald (PME) method within 0.9 nm and Grid algorithm was applied to calculate electrostatic interactions and search neighbors. Cutoff of 0.9 nm was used for Lennard-Jones and van der Waals interactions. Position restraints on the protein and ligand were used for system equilibrium during 1 ns. Table 1 provides detail of studied system. Simulations were repeated two times and averaged results were presented.

Table 1. Summary of studied systems.

No	System	No. water	T (K)
1	HSA-Ligand	8282	300
2	HSA-Ligand	8282	310

Diffusion coefficient

The mean displacement traveled by a molecule is called Mean square displacement (MSD). Einstein relation was used to calculate the self-diffusion coefficient D_A of particle A:

$$MSD = R(t) = \langle \|r_i(t) - r_i(0)\|^2 \rangle$$

$$\lim_{t\to\infty} \langle \|r_i(t) - r_i(0)\|^2 \rangle_{i\in A} = 6D_A t$$

The traveled distance by molecule i during time is $r_i(t) - r_i(0)$ that is averaged. The limiting slope of msd (t), vs. 6t is the D_A [20].

Potential of mean force

The equation used to calculate potential of mean force (PMF) was:

$$PMF = -K_B T \ln(r)$$

Where K_B, T *and* $g(r)$ are the Boltzmann constant, temperature, and radial distribution function (RDF) respectively [21].

Linear interaction energy (LIE)

The free energy of binding of ligand to HSA was computed by LIE algorithm at

two temperatures of 300 and 310 K. The LIE method divides the interaction between protein and ligand into electrostatic and van der Waals terms as follow:

$$\Delta G_{\text{binding}} = \alpha\left(\langle V_{l-s}^{\text{vdW}}\rangle_{\text{bound}} - \langle V_{l-s}^{\text{vdW}}\rangle_{\text{free}}\right) + \beta\left(\langle V_{l-s}^{\text{el}}\rangle_{\text{bound}} - \langle V_{l-s}^{\text{el}}\rangle_{\text{free}}\right) + \gamma \quad (4)$$

where $\langle V_{l-s}^{\text{el}}\rangle_{\text{bound}}$ and $\langle V_{l-s}^{\text{vdW}}\rangle_{\text{bound}}$ are the average electrostatic and van der Waals interaction energies between the ligand and the solvated protein from an molecular dynamics (MD) trajectory with ligand bound to protein and $\langle V_{l-s}^{\text{el}}\rangle_{\text{free}}$ and $\langle V_{l-s}^{\text{vdW}}\rangle_{\text{free}}$ are the average electrostatic and van der Waals interaction energies between the ligand and the water from an MD trajectory with the ligand in water. The value of α=0.5 came from the first order approximation of electrostatic contribution to the binding free energy. γ is a constant term obtained by regression fitting that gives absolute binding free energies. The results from LIE calculations, using the earlier optimized model of Hansson et al. [22] with γ=0, give relative binding free energies that agree very well with the experimental binding data. We have used the linear correlation between the value of β and WNDR to calculate this parameter. We then used this observed linear correlation to calculate the binding free energies for system with Ethyl 2-[2-(dimethylamino)-4-(4-nitrophenyl)-1,3-thiazole-5-yl]-2-oxoacetate and HSA at two temperature to compare the binding energies of them.

When protein and ligand bind to each other, the solvent accessible surface (SAS) of the ligand is smaller than the sum of SAS of protein and ligand before binding, because part of the protein and ligand which are exposed to water in free states are buried upon binding. The loss of the SAS due to binding was termed as the total desolvation SAS (tdSAS):

$$tdSAS = SAS_{complex} - (SAS_{protein} + SAS_{ligand}) \quad (5)$$

Obviously, the total desolvation solvent accessible surface of atom i (tdSASi) due to binding was calculated as:

$$tdSAS^{i} = SAS^{i}{}_{complex} - (SAS^{i}{}_{protein} + SAS^{i}{}_{ligand}) \quad (6)$$

where *i* = C, N, O and S, following the atom classes defined by Eisenberg and McLachlan [23]. The non-polar desolvation ratio (NDR) is defined as the ratio of total desolvation SAS of all nonpolar groups ($tdSAS^{i}$) where i are non polar groups, to the total desolvation SAS (tdSAS).

$$NDR = \frac{\sum_i tdSAS^{i}}{tdSAS} \quad (7)$$

The linear correlation between the value of β and NDR [23] was used to calculate β parameter.

Ligand Docking

Autodock 3.0 was used to calculate binding free energy between ligand and HSA. The structure of ligand was first drawn and optimized by Hyperchem. Then special changes were made in ligand structure such as polar hydrogens and Gasteiger charges were added to ligand; AutoTors tool was used to create the rigid root and rotatable bonds. Changes were also added to protein structure by autodock tool such as kollman charges and solvation parameters. Grid map was created around protein with dimension of 256 × 256 × 256 points using the Auto Grid tool. The 250 runs of genetic algorithm (GA) were adjusted with population size of 150, maximum number of 2.5×10^5 energy evaluations, maximum number of 27,000 generations, an elitism of 1, a mutation rate of 0.02, and a crossover rate of 0.8. Root-mean-square deviation (RMSD) of 0.5 was used to cluster structure and the clusters were ranked according to their free energy.

Result and discussion

Analysis of denaturation data

In this paper we are reporting the interaction of synthesized ligand Ethyl 2-[2-(dimethylamino)-4-(4-nitrophenyl)-1,3-thiazole-5-yl]-2-oxoacetate (Scheme1) with human serum albumin by applying isothermal titration UV-visible spectrophotometry. Also, we have determined the binding and thermodynamic parameters by analyzing the results.

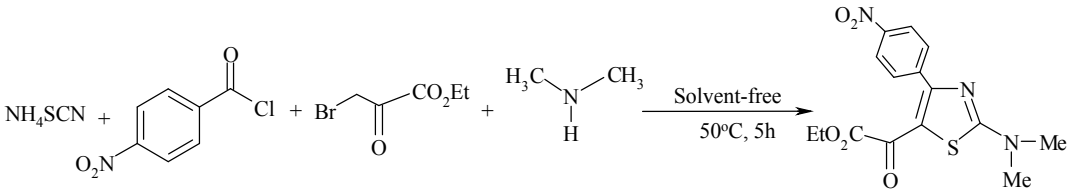

Scheme 1. Synthesis of Ethyl 2-[2-(dimethylamino)-4-(4-nitrophenyl)-1,3-thiazole-5-yl]-2-oxoacetate.

Effecting low concentration of ligand, HSA was denaturized. The profile of the HSA denaturation by ligand at different temperature of 27 and 37° C are shown in Figure 1, which related to two processes simultaneously: (1) ligand binding to the protein; (2) the protein denaturation. The concentration of ligand in the midpoint of transition, $[L]_{1/2}$, is low decreased by improving temperature, from 6.7 μmol/L at 27°C to 5.9 μmol/L at 37°C. So, the increasing of temperature was leading to the decrease in stability of the protein against denaturation caused by this ligand.

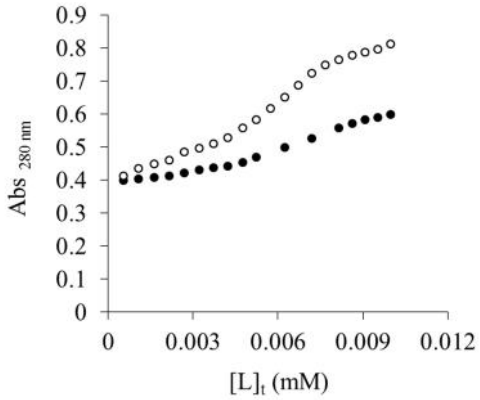

Figure 1. The changes of absorbance of HSA (0.8 mg/ml) at λ_{max}=280 nm due to increasing the total concentration of ligand, $[L]_t$, at 27 °C (•) and 37 °C (o).

Moreover, using Pace method [7], the thermodynamic parameters can be found in the process of HSA denaturation as reported earlier [8]. The values of the standard Gibbs free energy, the standard enthalpy and the entropy of protein unfolding, at 27° C and 37° C in the presence of ligand were calculated. The free energy of unfolding HSA with ligand which be decreasing by ligand addition (Figure 2).

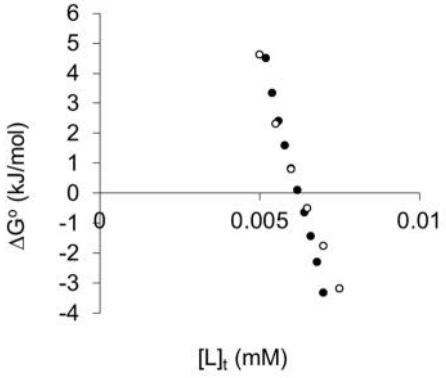

Figure 2. The standard Gibbs free energy plots of HSA unfolding (ΔG° vs. $[L]_t$) in the presence of ligand at 27 °C (•) and 37 °C (o).

Also, the heat needed for this protein unfolding is shown in the enthalpy curve of HSA denaturation in different concentration of ligand (Figure 3).

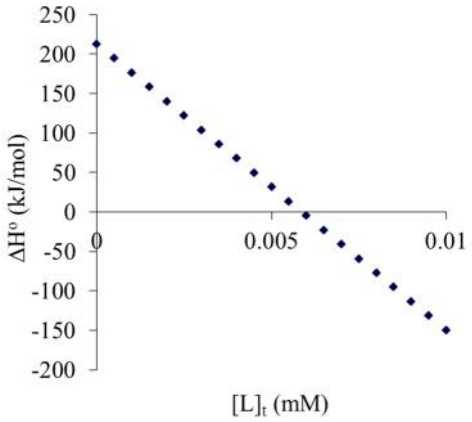

Figure 3. The molar enthalpy curve of HSA denaturation is due to the interaction with ligand in the range of 27 °C to 37 °C.

The obtained HSA denaturation data are summarized in Table 2. The positive value of entropy change related to the more disorder of denatured protein respect to the native protein.

Table 2. Thermodynamic parameters of HSA denaturation by ligand.

Temperature	$[L]_{1/2}$ [a] (μmol/L)	m [b] (kJ/mol)(mmol/L)$^{-1}$	ΔG°_{H2O} [c] (kJ/mol)	ΔH°_{H2O} [d] (kJ/mol)	ΔS°_{H2O} [f] (kJ/molK)
27° C	6.7	4.1	25.7	212.5	6.2
37° C	5.9	3.1	19.5	212.5	6.2

[a] The concentration of ligand in the midpoint of transition,
[b] Measure of ligand ability to denature HSA
[c] Conformational stability of HSA in the absence of ligand
[d] The heat needed for HSA unfolding in the absence of ligand
[f] the entropy of HSA denaturation by ligand

Binding parameters data

The results of isothermal titration indicate that the binding of ligand to HSA is positive cooperative. Titrating fixed amount of ligand with increasing concentration of HSA, at 27 °C and 37 °C, separately, ΔA_{max}, when all the binding sites on HSA were occupied by ligand, could be obtained from Figure 4.

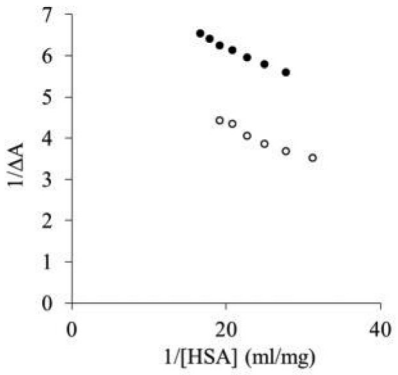

Figure 4. Scatchard plos, ν , the average number of bound ligand to one macromolecule of HSA; $[L]_f$, the free concentration of ligand (mmol/L) at 27 °C (●) and 37 °C (o).

Next, titrating fixed amount of protein with varying amount of ligand, binding parameters were calculated for the interaction of ligand with HSA at 27 and 37 °C. In this case, using binding data ($\bar{\nu}$, $[L]_f$), the Scatchard curves were plotted in Figure 5. Therefore, the binding of ligand to HSA are cooperative at both temperatures [9].

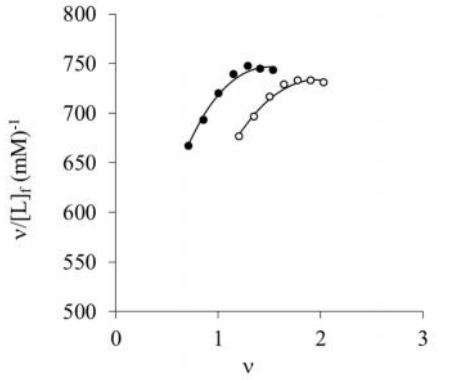

Figure 5. The changes in the absorbance of fixed amount of ligand in the interaction with varying amount of HSA at 300 nm at 27 °C (•) and 37 °C (o).

The binding data for the binding of ligand to HSA shown in Table 3, have been fitted to Hill equation using Eureka software, a computer program, for determining the theoretical values of these parameters. There is a set of 4 binding sites for ligand on HSA at 27 and 37 °C. The Hill coefficients at 27 and 37 °C are 1.6 and 1.9, respectively. So the cooperatively of binding is positive. Moreover, the values of the apparent equilibrium constant, K, indicate that the interaction affinity of ligand to HSA is near at 27 and 37 °C.

Table3. The binding parameters for the interaction of HSA with ligand in 10 mmol/L Tris-HCl buffer and pH 7.4.

Temperature	ΔA_{max} [a]	g [b]	K(mol/L)$^{-1}$ [c]	n [d]	Error [e]
27° C	0.126	4	362.1	1. 6	0.009
37° C	0.168	4	366.8	1.96	0.01

[a] Change in the absorbance when all the binding sites on HSA were occupied by ligand
[b] The number of binding sites
[c] The apparent binding constant
[d] The Hill coefficient
[e] Maximum error between theoretical and experimental values of $\bar{\nu}$

Finding the area under the binding isotherms plot (the values of $\bar{\nu}$ versus of the values of $Ln[L]_f$) for ligand of thiazol derivatives on HSA at both temperatures and using Wyman-Jons equation,[6] we can calculate the K_{app} and ΔG^o_b at 27 and 37 °C for each particular υ and also ΔH^o_b. Plots of the values of versus the values of $[L]_f$ are shown in Figure 6 at 27 °C. Deflection is observed clearly. This deflection indicates that at particular $[L]_f$, there is a sudden change in enthalpy of binding which may be due to binding of ligand to protein or protein denaturation.

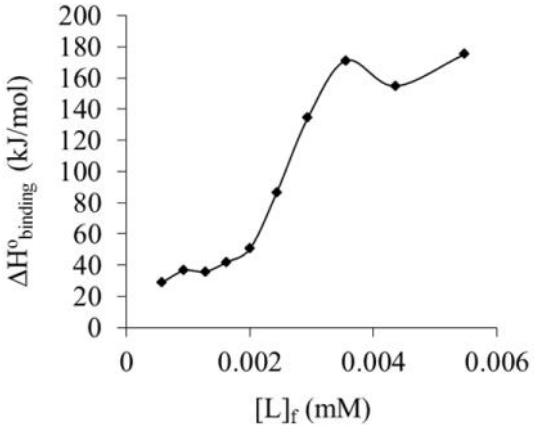

Figure 6. The molar enthalpies of the HSA interaction with ligand, is related to two processes simultaneously: (1) ligand binding to the HSA; (2) HSA denaturation at pH 7.4 and 27°C.

Fluorescence studies of synthesized ligand with HSA

As can be seen in Figure 7, the fluorescence intensity of HSA decreased regularly upon each addition of ligand in pH 7.4 and at room temperature. The emission of HSA is characterized by a broad emission band at 350 nm. Quenching fluorescence intensity of HSA gradually with the increase of ligand concentrations, the conformation of HSA containing internal fluorophores, such as Trp residues changed during the binding of ligand because chromophores of proteins are particularly sensitive to their microenvironment.

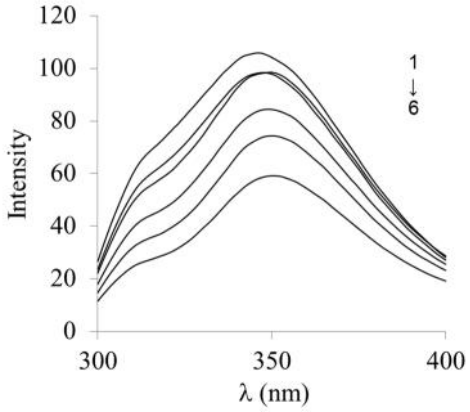

Figure 7. Fluorescence spectra of HSA interaction with ligand at room temperature. The concentration of HSA is 5 μM and the concentration of ligand (1) 0; (2) 2.5 μM; (3) 5 μM; (4) 7.5 μM; (5) 10 μM; (6) 12.5 μM, (pH=7.4).

Due to protein denaturation, ligand binding or conformational transition, the intensity in fluorescence emission spectra of Tryptophan (Trp) change. Hence, each molecular interaction of protein can result in quenching, which, the different mechanisms of quenching are usually

classified as either dynamic or static [24, 25]. The investigation of the quenching mechanism was done by Stern–Volmer equation (F0/F = 1 + Kq τ0 [L] = 1 + KSV [L]) where F0 and F are the fluorescence intensities in absence and presence of quencher, respectively, [L] is the quencher concentration, and Ksv is dynamic Stern–Volmer quenching constant, which can be written as Kq = Ksv/τ0, where Kq is the biomolecular quenching rate constant and so is the average lifetime of the fluorophore (Trp-214) in absence of quencher and its value is around 10-8 s for most biomolecules. Therefore, from the plot of F0/F versus [L], Ksv was determined 0.177 (M^{-1}) and Kq value was $1.7\times107(Ms)^{-1}$ that was lower than the maximum scattering Energy transfer between various quenchers and biopolymers collisional quenching, 2.0×10^{10} $(Ms)^{-1}$. Consequently, a dynamic quenching mechanism was the possible predominance of in the HSA–ligand formation.

In addition, the binding constant of ligand with HSA (Kb) and the number of binding sites (g) can be obtained from Equation of log (F0–F/F) = logKb + g log[L]. The experimental values of log (F0–F/F) were plotted as a function log[L] of to give a good straight line (figure 7b), the g=2.6 and Kb= $6.1\times1017(M^{-1})$ were obtained from the slope and antilog of intercept through the straight line, respectively.

Molecular dynamics simulation

According to [26], total and potential energies are useful quantities to determine system equilibrium after position restraining the ligand and HSA structure. Figure 8a depicts the potential energy of systems after interaction at 310 and 300 K. The nearly constant potential energy curves appeared in this figure. At lower temperatures, our system has less mobility and kinetic energy and more negative potential energy [26]. Therefore it can be concluded that HSA-ligand has negative potential energy and more stability at lower temperature.

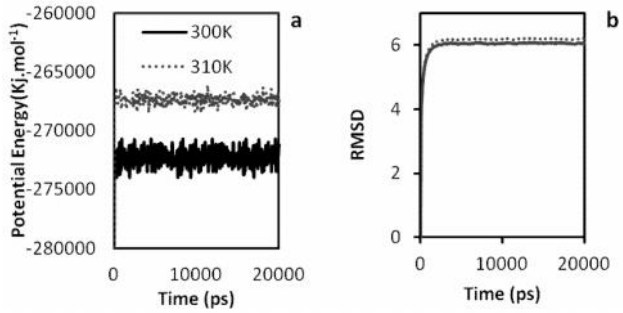

Figure 8 a-b. Potential energy of both studied system b) Root mean square deviation (RMSD) of the HSA in the presence of ligand at two temperatures (In all part of simulation data, blue color denotes 300 K and red color denotes 310K).

Figure 8b shows RMSD of the HSA-ligand during 20 ns. It shows that the structure deviation of HSA reaches a stable state after 2 ns. It also shows that HSA has more mean square deviation at higher temperature. Figures 8c and 8d report the temperature and pressure curves of two systems as well as the steady state in these parameters that also confirms equilibrium in an NPT ensemble.

Variation of hydrogen bond between HSA and solvent during 20 ns was studied and results are depicted in Figure 9a. Results display that increase of temperature was followed by a decrease in the hydrogen bond that is due to ligand effect on structure of HSA and ligand cause solvent molecule exclusion from protein and this effect increase upon temperature increase.

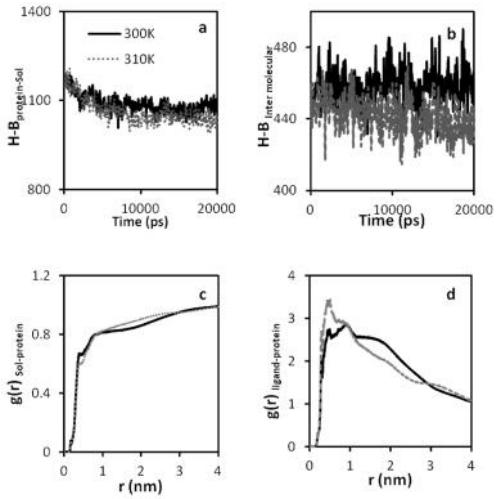

Figure 9a-d. a)Variation of hydrogen bond (H-B) between HSA and solvent b) intermolecular hydrogen bond of HSA c) The RDF of ligand-HSA d) The RDF of solvent-HSA

Figure 9b shows intermolecular hydrogen bond of HSA at 300 and 310 K. Results of this figure proves decrease of HSA intermolecular hydrogen bond at higher temperature and this decrease may be due to more denaturation or unfolding of HSA structure at 310 K. Figure 9c displays the RDF of ligand around HSA. It confirms more RDF at 310 K. More RDF of ligand-HSA at 310 K is in good consistency with less intermolecular hydrogen bond of HSA. Figure 9d depicts RDF of solvent-HSA at two temperatures. It is found that probability of finding solvent around HSA decrease by temperature. At 310 K, ligand excludes solvent from HSA surface more due to more interaction between ligand and protein. It means that a hydration layer can be considered around HSA surface that after interaction, this hydration layer change and ligand replaces solvent molecule in this layer and cause protein denaturation [27]. The surface area of HSA obtained and Figure 10 shows the

hydrophobic (10a) hydrophilic (10b) and total (10c) solvent accessible surface area of HSA during 20 ns. Results show that surface area of HSA increases with temperature. It reveals that HSA has been unfolded more by ligand at 310 K.

Figure 10d shows the radius gyration of HSA. This figure shows increase of radius gyration of HSA at 310K. The increase in radius gyration is accompanied with increase of hydrophobic surface area of HSA at 310 K that proves HSA denaturation.

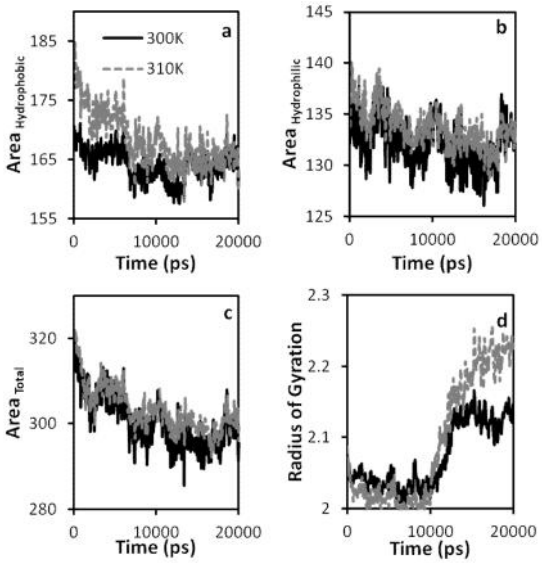

Figure 10a-d. The variation of the a) hydrophobic b) hydrophilic c) and total surface area d) and the gyration radius of HSA

Figure 11 shows the PMF profile. This figure shows that after ligand reaching to the HSA, system becomes unstable and PMF increases. At higher temperature the system is more unstable and PMF increases. The minimum distance in the PMF curve is (-3.18 nm) at 300K and (-2.47) at 310 K and the minimum depth decreases at 310K. Our results indicate stabilization of system at 300K. It means that protein and ligand are in more favorable and stable environment at lower temperature.

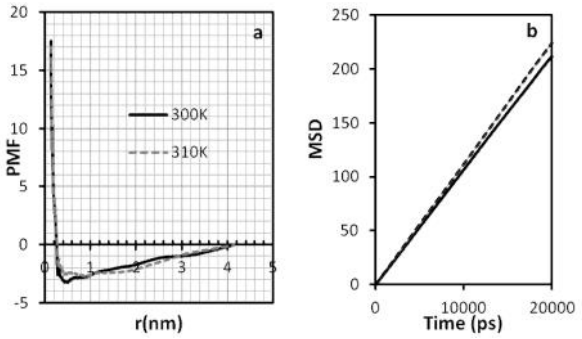

Figure 11a-b. a) The profile of the PMF b) MSD of ligand at two temperatures.

Figure 11b shows the MSD of ligand at 300 and 310 K. Results show less travel of distance by ligand at lower temperature that is the reason for less protein denaturation. Values of DA that are slope of MSD curves are tabulated in Table 4. Based on DA values, ligand molecule travels more distance to protein at higher temperature. DA increases with temperature that implies to more mobility of ligand and more instability of system at 310 K.

Table 4. Values of D_A for two systems at 310 and 300 K.

No	D_A	T (K)
1	0.001767	300
2	0.001867	310

VADAR [28] website was used to calculate structural files of helix and coil sheets for HSA in two systems at 300 and 310 K. HSA helix and coil structures are depicted in Fig. 12a and b. Helix content is decreased and coil structure is increased more at higher temperature, which confirms more HSA denaturation. Thus, the ligand interact with HSA and decrease the helix content by denaturing the structure and this denaturation is more at higher temperatures.

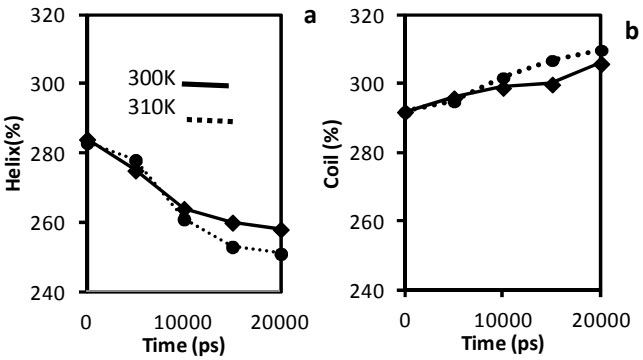

Figure 12. a) Variation of helix and b) coil structure for HSA at 300 and 310 K.

Time-coursed snapshots of the system at 310K depicted in Figure 12 indicate interaction process of ligand with protein. At the beginning of simulation (before simulation) the ligands locate around the protein and after simulation (20ns) ligands came near the protein and interact with it.

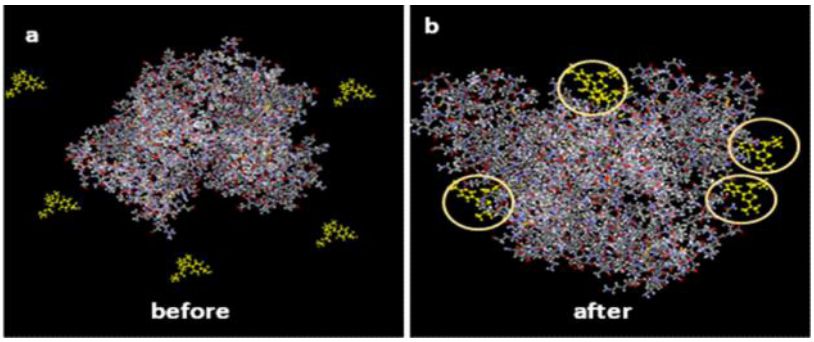

Figure 13. Time-coursed snapshots of the system at 310K before (0ns) and after simulation 20ns.

The electrostatic and van der Waals contributions to the free energy difference are given in Table 5 with β=0.27 calculated from NDR [23] diagram.

Table 5. Free energy values of the systems obtained from LIE method.

system	Bounded (kJ mol^{-1})		Free (kJ mol^{-1})		Free Energy (kJ mol^{-1})
	L-J	VDW	L-J	VDW	
310 K	-814.7	-356.6	-925.1	-231.5	-32.75
300 K	-762.0	-372.3	-814.1	-290.4	-26.88

When the ligand interacts stronger with protein, the Gibbs free energy is more negative. It reveals that ligand bind to HSA with a binding energy of -32.75 and -26.88 kJ mol^{-1} at 310 and 300 K respectively. The most negative value of free energy is at higher temperature and it may be the reason and confirm for more denaturation and more reduction of helix structure or reduction of intermolecular hydrogen bonding of HSA at higher temperature. The high and negative value of electrostatic energies compared to van der waals energies reveals that may be the main forces contributing to denaturation of HSA by ligand is due to electrostatic interaction [29, 30].

Molecular docking result

HSA structure optimized with molecular dynamic simulation and docked to ligand. Table 5 presents free energy of ligand docking to HSA according to sorted values. The negative value of Gibbs free energy (-11.15 kJ/mol) reveals the spontaneous process of ligand-protein interaction.

Table 6. Lowest docked energy for binding of studied ligand to HSA.

Cluster-rank	Lowest docked energy	Run	Mean docked energy
1	-11.15	42	-11.115
2	-11.08	180	-11.08
3	-10.93	33	-10.93
4	-10.90	154	-10.90
5	-10.89	193	-10.80

The interacted amino acids with HSA in the most negative binding site are presented in Figure 14. Based on the results presented in Figure 14, the most negative binding interaction between ligand and HSA placed within domain I so that ligand interacts with Arg 22, Arg 218, Lys 195, Lys 199, His 242, Arg 257 and Ala 291.

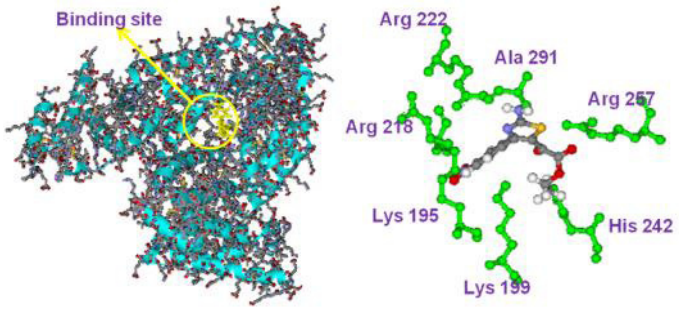

Figure 14. The closest interacted amino acid with ligand in the most negative binding site obtained from docking.

Conclusion

The analytical data and spectroscopic studies suggest that the synthesized ligand can denature HSA at low concentration. Also, increasing temperature has no influence on ligand efficiency in binding affinity with HSA. In addition, fluorescence spectra of this interaction revealed that conformation of HSA change in the binding micromolar concentration of ligand to protein with dynamic quenching mechanism. There are two binding sites for electrostatic and hydrophobic interaction with protein. On the basis of change in enthalpy of binding, it can be concluded that the synthesized ligand can denture the protein by exothermically binding including endothermically denaturation process. Also, it is expected that one of the side effects of drugs might be due to their interaction with carrier proteins as HSA. The molecular dynamic results also confirmed experimental results.

References

[1] B. Denny (Cancer Research Laboratory) and Heather Wansbrough and based on: Denny, William A.; *New Directions in Cancer Chemotherapy*; Chemistry in New Zealand (1995).

[2] William A. Denny, *The Design and Development of Anticancer Drugs*; Chemical Processes in New Zealand, edition one, volume two XII-*Biotech-J-Cancer Drugs-1*.

[3] F. Q. Cheng, Y. P. Wang, Z. P. Li, C. Dong, *Spectrochim. Acta Part A,* 65, 1144 (2006).

[4] F. Cui, J. Wang, Y. Cui, J. Fan, J. Li, X. Yao, *Anal. Sci.,* 23, 719 (2007).

[5] F. L. Cui, J. Fan, W. Li, Y. C. Fan, Z. D. Hu, *J. Pharm. Biomed. Anal*., 34, 189 (2004).

[6] P. Das, A. Mallick, B. Haldar, A. Chakrabarty, N. Chattopadhyay, *J. Chem. Sci.*, 119, 77 (2007).

[7] N. H. G. Holford, L. Z. Benet, B. G. Katzung. Basic and clinical pharmacology, 7th edn. Appleton and Lange, Stamford; (1998).

[8] T. C. Kwong, *Clin Chim Acta*. 151, 193 (1985).

[9] H. Kurz, New York: Praeger Publishers; 70 (1986).

[10] G. Ascoli, C. Bertucci, P. Salvadori, *J. Pharm Sci.*, 84, 737(1995).

[11] D. C. Carter, X. M. He, S. H. Munson, P. D. Twigg, K. M. Gernert, M. B. Broom, T.Y. Miller, *Science*, 244, 1195 (1989).

[12] D. J. Birkett, D.N. Wade, G. Sudlow, *Mol Pharmacol*., 12, 1052 (1976).

[14] H. Mansouri-Torshizi, M. Islami-Moghaddam, A. A. Saboury, Acta Biochimica et *Biophysica Sinica*., 35,886 (2003).

[14] R. F. Greene, C. N. Pace, *J. Biol. Chem.* 249(10), 5388 (1974).

[15] M. Islami-Moghaddam, H. Mansouri-Torshizi, A. Divsalar, A. A. Saboury, *J. Iran. Chem. Soc*., 6(3), 552 (2009).

[16] A. A. Saboury, *J. Iran. Chem. Soc.*, 3, 1 (2006).

[17] A. V. Hill, *The Journal of Physiology*, 40, 4 (1910).

[18] A. A. Saboury, A. A. Moosavi–Movahedi, H. Mansouri–Torshizi, *J. Chin. Chem. Soc.*, 46, 917 (1999).

[19] D. Van Der Spoel GROMACS: Fast, flexible, and free. *J. Comput. Chem*., 26, 1701 (2005).

20. M. P. Allen, D. J. Tildesley, Computer Simulations of Liquids. Oxford: Oxford Science Publications (1987).

[21] F. Mehrnejad, M. M. Ghahremanpour, M. Khadem-Maaref, F. Doustdar *J. Chem. Phys.,* 134, 035104 (2011).

[22]. T. Hansson, J. Marelius, J. Aqvist, J, *J. Comput.*Aided Mol. Des., 12, 27 (1998).

[23] D. Eisenberg, A. D. McLachlan, *Nature*, 319, 199 (1986).

[24] MacManus-Spencer, *Anal. Chem*., 82(3), 974 (2010).

[25] Hebert and MacManus-Spencer, *Anal. Chem*., 82(15), 6463 (2010).

[26] C. Rungnim, U. Arsawang, T. Rungrotmongkol, S. Hannongbua, *Chem. Phys. Lett.,* 550, 99 (2012).

[27] A. A. Saboury, A. K. Bordbar, A. A. Moosavi-Movahedi, Bull. *Chem. Soc. Jp*, 69, 3031 (1996).

[28] http://redpoll.pharmacy.ualberta.ca/vadar.

[29] A. A. Moosavi-Movahedi, A. A. Saboury, *J. Chem. Soc. Pak.*, 21, 248 (1999).

[30] A.A. Saboury, *J. Iran. Chem, Soc.,* 6, 219 (2009).